Current Biology, Vol. 15, 1979–1988, November 22, 2005, ©2005 Elsevier Ltd All rights reserved. DOI 10.1016/j.cub.2005.09.054

Length Control of the Metaphase Spindle

Gohta Goshima,[1,2,4] Roy Wollman,[1,3,4] Nico Stuurman,[1,2] Jonathan M. Scholey,[3] and Ronald D. Vale[1,2,*]
[1] Physiology Course 2004
Marine Biological Laboratory
Woods Hole, Massachusetts 02543
[2] The Howard Hughes Medical Institute and
Department of Cellular and Molecular Pharmacology
University of California, San Francisco
San Francisco, California 94143
[3] Department of Molecular and Cellular Biology
University of California, Davis
Davis, California 95616

Summary

Background: The pole-to-pole distance of the metaphase spindle is reasonably constant in a given cell type; in the case of vertebrate female oocytes, this steady-state length can be maintained for substantial lengths of time, during which time microtubules remain highly dynamic. Although a number of molecular perturbations have been shown to influence spindle length, a global understanding of the factors that determine metaphase spindle length has not been achieved.
Results: Using the *Drosophila* S2 cell line, we depleted or overexpressed proteins that either generate sliding forces between spindle microtubules (Kinesin-5, Kinesin-14, dynein), promote microtubule polymerization (EB1, Mast/Orbit [CLASP], Minispindles [Dis1/XMAP215/TOG]) or depolymerization (Kinesin-8, Kinesin-13), or mediate sister-chromatid cohesion (Rad21) in order to explore how these forces influence spindle length. Using high-throughput automated microscopy and semiautomated image analyses of >4000 spindles, we found a reduction in spindle size after RNAi of microtubule-polymerizing factors or overexpression of Kinesin-8, whereas longer spindles resulted from the knockdown of Rad21, Kinesin-8, or Kinesin-13. In contrast, and differing from previous reports, bipolar spindle length is relatively insensitive to increases in motor-generated sliding forces. However, an ultrasensitive monopolar-to-bipolar transition in spindle architecture was observed at a critical concentration of the Kinesin-5 sliding motor. These observations could be explained by a quantitative model that proposes a coupling between microtubule depolymerization rates and microtubule sliding forces.
Conclusions: By integrating extensive RNAi with high-throughput image-processing methodology and mathematical modeling, we reach to a conclusion that metaphase spindle length is sensitive to alterations in microtubule dynamics and sister-chromatid cohesion, but robust against alterations of microtubule sliding force.

*Correspondence: vale@cmp.ucsf.edu
[4] These authors contributed equally to this work.

Introduction

Microtubules (MTs) are highly dynamic polymers that continually change their length by growth or shrinkage [1]. Remarkably, whereas individual MTs fluctuate in length, the ensemble of microtubules in the mitotic spindle maintains a constant spindle length throughout metaphase [2]. Several studies using various experimental systems from yeast to humans have shown that spindle length can be influenced by changes in MT polymer dynamics, mitotic motor activity, or sister-chromatid cohesion [3–11]. However, a systematic and quantitative analysis of the factors that establish and maintain the steady-state spindle length at metaphase has not been performed. Moreover, studies on the consequences of perturbations of individual proteins on metaphase spindle length are often not consistent among different experimental systems. For example, alterations in MT length by inhibition of MT-dynamics regulators directly affect spindle length in some systems (e.g., [3, 11]) but not in others [9]. A quantitative assessment of the contributions of different force generators to spindle length in a single cell type would greatly aid efforts to understand and potentially computationally model the balance of forces acting to maintain the length of the metaphase spindle [12–14].

The *Drosophila* S2 cell line is a good animal cell for investigating spindle-length control, because it has a diamond-shaped spindle that has similar morphological features to somatic vertebrate cells and because a number of conserved proteins that affect spindle morphology have been identified by RNAi-based functional analyses [3, 4, 15–17]. In this study, we determined metaphase spindle length after RNAi knockdown and/or overexpression of factors that mediate MT sliding, MT dynamics, or sister-chromatid cohesion. We examined the following proteins whose mitotic phenotypes after RNAi depletion and, in most cases, in vitro molecular activities have been characterized. To modulate MT sliding, we focused on Klp61F (Kinesin-5), a conserved, bipolar, plus-end-directed kinesin that is thought to generate outward sliding forces between antiparallel MTs and would be expected to elongate the spindle. Indeed, previous studies in yeast have shown that overproduction or reduction of Kinesin-5 causes metaphase spindle lengthening or shortening, respectively [5, 7]. We also examined two minus-end-directed motors, Kinesin-14 (Ncd in *Drosophila*) and cytoplasmic DHC (Dhc64C), because these motors could influence metaphase spindle length by generating an inward sliding force that opposes the actions of Kinesin-5 [5, 6, 8, 9, 18] (in some cells, dynein could also augment Kinesin-5 by pulling astral MTs toward the cell cortex [19]). To explore factors that influence MT dynamics, we examined three proteins that promote MT assembly at the MT plus end: the plus-end-tracking protein EB1 [16], Msps [Dis1/XMAP215/TOG] [20], and Mast/Orbit [CLASP] [17, 21], as well as the MT-depolymerizing factor, Klp10A (Kinesin-13) [3, 4], and the putative depolymerizer Klp67A (Kinesin-8) [3, 22–24]. The actions of Mast/Orbit and Klp67A are thought to be

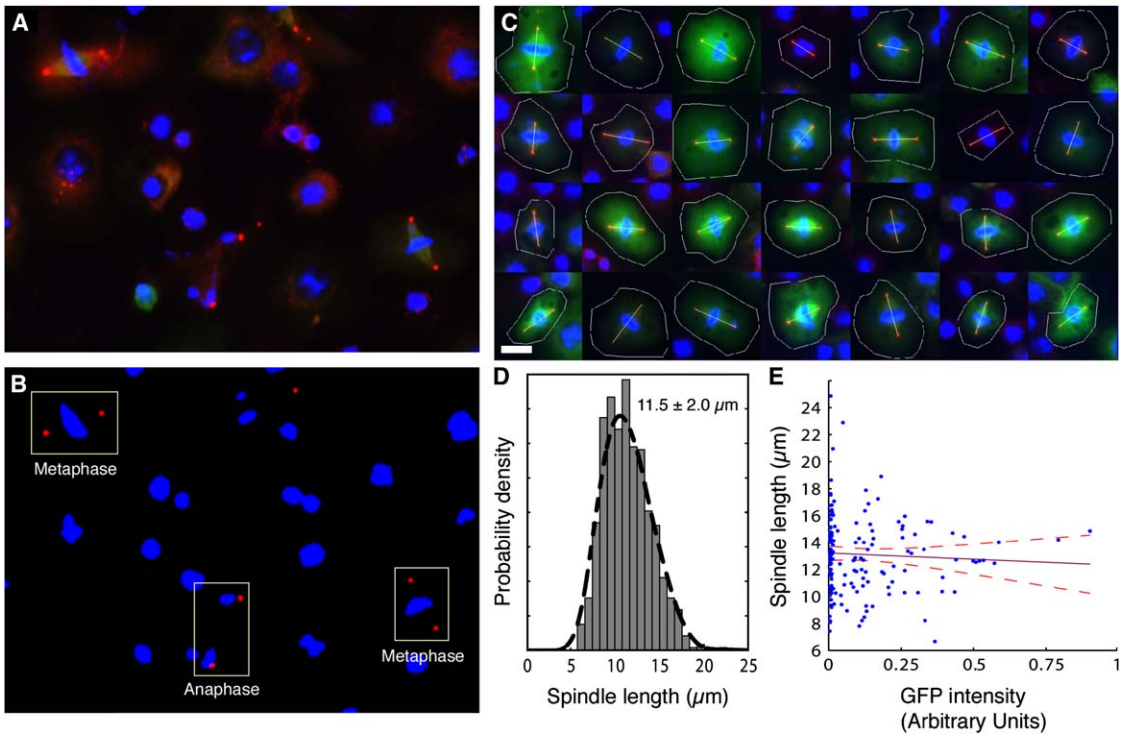

Figure 1. High-Throughput, Semiautomated Measurement of Metaphase Spindle Length of *Drosophila* S2 Cells

(A) A raw image taken by the automated ImageXpress microscope with a 40× objective. Control GFP-tubulin cells were stained with γ-tubulin (red) and chromosomes (blue). GFP is shown in green.

(B) Enhanced signals of γ-tubulin and chromosomes (see Supplemental Experimental Procedures). Two metaphase cells and one anaphase cell were detected by the existence of two γ-tubulin signals and chromosome masses in between. Most of the interphase cells were not stained by γ-tubulin antibody.

(C) A gallery of metaphase cells. After automated detection of γ-tubulin-stained cells, all the nonmetaphase cells were eliminated by manual selection. Cell shape was estimated by the boundary of the diffuse GFP signals in the cytoplasm (white circle), and GFP expression level was quantified as the signal intensity within the area. The bar represents 10 μm.

(D) Distribution of metaphase spindle length of control GFP-tubulin cells. Data from 703 mitotic cells were combined. Average length (11.5 ± 2.0 μm) was well reproduced in each experiment (see Table S1).

(E) Spindle length was plotted against GFP intensity. No statistically significant correlation was found between GFP level and spindle length, indicating that GFP-tubulin expression itself did not perturb the spindle.

exerted primarily at kinetochores [17, 21–24]. Klp10A and EB1, on the other hand, are concentrated at the centrosome, although both are likely to modulate MT assembly throughout the mitotic cytoplasm as well [3, 4, 16]. To interfere with sister-chromosome tension, we depleted the critical sister-chromatid-cohesion protein, Rad21 (cohesin) [15]. Our results show that modulators of MT dynamics and chromatid cohesion are the major governors of spindle length. In contrast, bipolar spindle length is robust to changes in MT sliding forces produced by the Kinesin-5. We produce a mathematical model that provides a framework for understanding these observations.

Results and Discussion

Mitotic cells are relatively rare in the S2-cell population (1%–3%). Therefore, we required a method to obtain images of sufficient numbers of mitotic spindles for quantitation and statistical comparison among different RNAi treatments. In most cases, we employed a high-throughput procedure of image collection and analysis, as summarized below and in Figure 1 (and Figure S1 in the Supplemental Data available with this article online) for control GFP-tubulin-expressing cells [3]. Cells were plated onto concanavalin-A-coated, 96-well glass-bottom dishes and then fixed and stained for γ-tubulin (as a marker of centrosome locations) and chromosomes (Figure 1A). For the majority of our experiments, images were collected with a high-throughput automated microscope, and a semiautomated image-analysis procedure was used to identify the rare mitotic cells in the images. This algorithm, which took advantage of the fact that most interphase S2 cells do not exhibit punctuate signals of γ-tubulin [3], recognizes γ-tubulin spots and identifies a cell as mitotic if it contains a pair of γ-tubulin spots with a DAPI-staining chromosomal mass in between (Figure 1B). During this process, γ-tubulin spot–spot distances were measured automatically. Potential metaphase cells were then displayed into visual galleries, and a manual selection was performed to eliminate prophase, anaphase, and aberrant interphase cells as well as metaphase cells with multipolar spindles, which had been also selected by the automated selection process (see Figure S1 for an example of manual selection). The average distribution of the spindle length (herein defined as centrosome-to-centrosome distance) in 703 control cells from several experiments was 11.5 ± 2.0 μm

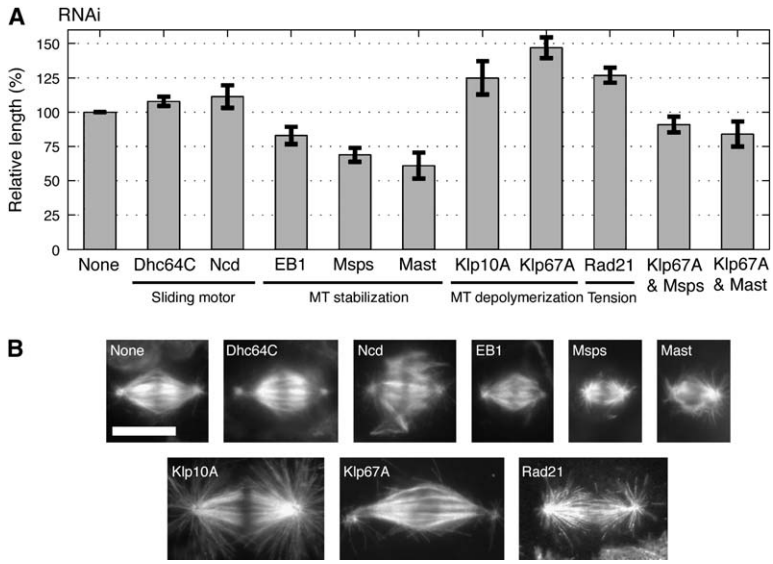

Figure 2. Metaphase Spindle Length after RNAi

(A) Average length of metaphase spindle after single or double RNAi-knockdown of eight proteins. RNAi treatment of each gene was repeated at least once, and in each experiment, relative average length to the accompanying control was obtained. Combined dataset of all the treatments is described in this graph. Error bars represent the 95% confident interval. See Table S1 for individual datasets.

(B) Representative spindle images after RNAi of indicated genes. These images were taken manually with a 63× oil immersion objective. The bar represents 10 μm.

(Figure 1D). This length distribution was broader than those observed in yeast or fly embryos [6, 10]. However, using a sufficient sample, we obtained consistent average metaphase spindle length among experiments (10.95–11.84 μm; Table S1). By plotting spindle length versus GFP intensity for individual cells, we also established that the spindle length was independent of GFP-tubulin expression levels (Figure 1E).

Next, we applied the same procedure to examine metaphase spindle length in cells depleted of various proteins by RNAi (Figure 2; see also Table S1 for statistical summary). One general caveat of RNAi approach is that the targeted proteins are not completely depleted and that the observed phenotypes (especially "no phenotype") could be still "hypomorphic" as a result of the residual proteins. Although this is also the case of our study, we confirmed significant protein-level reduction for most of the genes (Figure S2A) and could observe specific spindle/chromosome phenotypes (Figure 2B). First, we found that reduction of Rad21, a protein essential for sister-chromatid cohesion, led to longer spindles, as documented in yeast [10]. After Rad21 RNAi, anti-Cid staining (an inner-kinetochore marker) revealed no paired sister-kinetochore dots, and thin chromosomal masses were scattered, strongly suggesting the precocious separation of sister chromatids (Figure S4A) [15]. Statistically significant effects also were observed for regulators of MT dynamics. In agreement with previous qualitative descriptions [3, 4, 16, 17, 25], RNAi of the MT stabilizers EB1, Msps, and Mast caused shortening of metaphase spindle (61%–83%; all p values < 0.0007), whereas knockdowns of MT depolymerases (Klp10A and Klp67A) caused expansion (125%–147%, all p values < 0.004). Notably, the outer-kinetochore-enriched regulators of MT plus ends (Klp67A, Mast) affected the length more severely than the global or centrosome-localized MT regulators EB1, Msps, and Klp10A. Klp67A [3] and EB1 [16] RNAi sometimes causes centrosome detachment from the kinetochore microtubules (kMTs), and this detachment could skew our measured centrosome-to-centrosome distance from the actual spindle length. However, the degree of centrosome separation from the kMT for EB1 RNAi is small, only accounting for a 0.2 μm increase to the measurement of spindle length [26]. In the case of Klp67A, the centrosome is detached, but is not always localized along the axis. Indeed, by comparing measurements of centrosome-to-centrosome distance to the distances of the minus ends of the kMT in 32 bipolar spindles, we find that the centrosome-to-centrosome distance in Klp67A RNAi cells underestimates spindle length by 0.3 μm compared with control cells. Nevertheless, these effects are small and do not affect our conclusions that EB1 and Klp67A RNAi treatments shorten and lengthen spindle length, respectively.

If spindle length is controlled by a balance of MT polymerization and depolymerization, we reasoned that a phenotype generated by depletion of the MT-depolymerizing protein Klp67A might be rescued by depletion of MT-polymerizing proteins (e.g., Msps or Mast). In accordance with this idea, the simultaneous knockdown of Klp67A and Msps or Mast produced an average length that was intermediate between single Klp67A and single Msps or Mast knockdowns (Figure 2A).

The important role played by MT-polymerization dynamics in determining spindle length was also discovered recently in *Xenopus* egg extracts by Mitchison and colleagues, who also argued that an unidentified non-MT tensile element, possibly a "spindle matrix" [27], may constrain spindle length [28]. Although we cannot exclude the existence of such an element, our results have not uncovered evidence for its existence. For example, shortening of MT length by EB1 or Msps RNAi produced short metaphase spindles without significantly perturbing its shape (Figure 2B).

Previous studies have shown that the inhibition of a minus-end-directed kinesin (Kinesin-14) causes spindle elongation in yeast [5, 8]. Dynein inhibition causes drastic spindle elongation or shortening depending upon the cell type [6, 9]. However, RNAi of Ncd (Kinesin 14) or Dhc64C (cytoplasmic DHC) only slightly changed the spindle size in S2 cells (3%–17% increase; Figure 2A and Table S1). The slight increase after dynein knockdown can be explained by the effect of detachment of

centrosomes from spindle poles [29, 30] because we recently found in another study that detachment of the centrosomes from the minus end of kMT alone accounts for an average 14% increase in the centrosome-to-centrosome distance [26]. The spindle-length increase after dynein RNAi is less than that observed by Morales-Mulia and Scholey [31], for reasons that are not clear. However, these authors also noted a partial misrecruitment of the Klp10A depolymerase to the poles, a misrecruitment that may have contributed to this effect. The lack of dramatic effect upon Ncd RNAi is unlikely to be due to residual proteins because we noted splaying of kinetochore fibers (a characteristic of Ncd RNAi knockdown [3, 26]) in the majority of the mitotic spindles examined (80%), found significant depletion (>90%) of Ncd at the population level by immunoblot analysis, and found that 33 of 36 mitotic spindles scored had no detectable immunofluorescence signal for Ncd after Ncd RNAi. However, the slight increase of the spindle length might be explained by the reduced spindle elasticity upon unfocusing of kinetochore fibers (discussed in Box 1). Depletion of Klp61F (Kinesin-5) by RNAi produced monopolar spindles [3], so the length of bipolar spindles was not a measurable parameter. Collectively, these quantitative comparisons of spindle length following RNAi-mediated protein depletion indicate that MT polymer dynamics and sister-chromatid cohesion more dramatically affect metaphase spindle length than depletion of minus-end-directed motor proteins.

We next examined whether increasing the levels of MT sliding motors (Klp61F, Ncd) or of MT depolymerases (Klp10A, Klp67A) influences spindle length (Figure 3). To correlate expression level and spindle length on a cell-to-cell basis, we expressed GFP-tagged kinesins from an inducible promoter (Figure 3B) and measured GFP levels and spindle lengths for individual cells. In support of our assumption that the exogenous fusion proteins are physiologically functional, we observed that moderate expression of these kinesin-GFP fusions rescued the loss-of-function spindle phenotypes produced by depletion of the corresponding endogenous kinesin by RNAi, and this rescue suggests that GFP tagging did not destroy the kinesin's function [22]. Moreover, overexpressed Klp67A-GFP localized primarily to kinetochores and kinetochore MTs (kMTs), and overexpressed Ncd-GFP and Klp61F-GFP localized primarily

Box 1. Mathematical Force-Balance Model of Metaphase Spindle-Length Control

Here, we outline a simple dynamical force-balance model of the determinants of S2-cell metaphase spindle length, a model that is a modification of an earlier quantitative model that explains spindle-pole dynamics during anaphase B [B1]. As described below, an important aspect of this model is that Kinesin-5-driven MT sliding activity is coupled to MT depolymerization, and this coupling guarantees stability of the steady-state solution and allows robustness of spindle stability to changes in MT dynamics.

We first define three state variables that are important for tracking spindle dynamics: spindle lengths (S), length of overlapping region of antiparallel MTs (L), and MT sliding velocity ($V_{sliding}$) (Figure A, left). In Figure A (right), we describe the total force acting directly on the centrosome. Outward force, $F_{sliding}$, is opposed by $F_{tension}$ and F_{kt}.

In addition, we define the following forces (1–3 below) and parameters of microtubule polymerization (4–5) relevant to the metaphase spindle (Figure A):

1. $F_{sliding}$ (green): The Kinesin-5-dependent force that slides apart antiparallel MTs (e.g., between antiparallel interpolar (ip) MTs or between ipMT and kMT [B2]) and acts to separate centrosomes and also on chromosomes through kMTs.
2. $F_{tension}$ (purple): Spindle elasticity, an assumed restoring force that behaves as a Hookean spring and opposes spindle extension (possibly MT elasticity, MT crosslinking, or a "spindle matrix").
3. F_{kt} (yellow): A force (in addition to $F_{sliding}$) that pulls the kinetochore toward the pole and pulls centrosomes inward (Figure B) and that could be due to Hill sleeve mechanism [B3], minus-end-directed motors at the kinetochore, or MT depolymerization at the pole.
4. V_{poly}: The rate of MT polymerization at the plus ends of antiparallel ipMTs as determined by dynamic instability of MTs and as a function

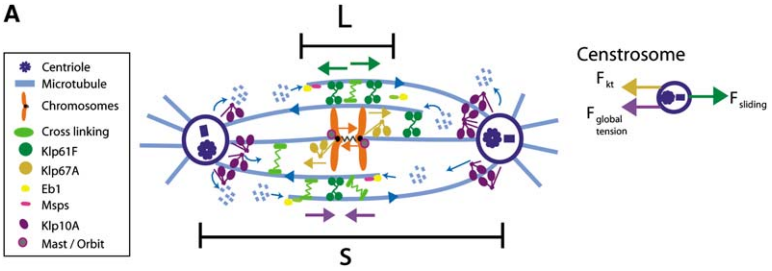

Figure A. Schematic Representation of the Forces Acting on the Metaphase Spindle

Continued on following page

of "general" MT regulators (e.g., EB1 or minispindles).

5. V_{depol}: The rate of depolymerization of all MTs at their minus ends, this may be mainly regulated by Kinesin-13 (Klp10A) that acts as a MT depolymerase.

Forces exerted by astral MTs [B4–B6] or chromokinesins [B7] may also play a role in spindle-length determination, but they were not considered in this study for simplicity. We do not take into account an eventual limitation of the size of the spindle (i.e., limited amount of tubulin or other spindle components or size of the cell), although these factors may also come into play in living cells.

The microtubule polymerization/depolymerization rates can be combined with the rate of MT sliding, $V_{sliding}$, to form two simple kinematic equations:

$$\frac{dS}{dt} = 2\left(V_{sliding} - V_{depol}\right) \quad (1)$$

$$\frac{dL}{dt} = 2\left(V_{poly} - V_{sliding}\right) \quad (2)$$

This set of kinematic equations should be coupled to a third force-balance equation, which is based on the low Reynold's number approximation that applies at subcellular scales (force for movement, F = velocity of movement, dS/dt × the drag coefficient of separating the poles, μ).

$$\frac{dS}{dt} = \mu^{-1} 2\left(F_{sliding} - F_{kt} - F_{tension}\right) \quad (3)$$

The above forces can be defined as follows:

$$F_{sliding} = \alpha L\left(1 - \frac{V_{sliding}}{V_{sliding,\,\max}}\right) \quad (4)$$

$$F_{tension} = \beta\left(S - S_0\right) \quad (5)$$

$$F_{kt} = F_{kt,0} \quad (6)$$

The sliding force parameter α represents Kinesin-5 force per unit length of overlap (L) ($pN/\mu m$), and $V_{sliding,\,\max}$ is the maximal unloaded MT sliding velocity of Kinesin-5. β is the Hookean-spring constant of spindle elasticity, and S_0 is the spring's rest length. For simplicity, we assume a constant force on the kinetochore ($F_{kt,0}$). The assumption of linear force-extension forces for the spindle spring elements and of linear force-velocity curves for Kinesin-5 activity serve to simplify the system and ensure the existence of analytical solutions.

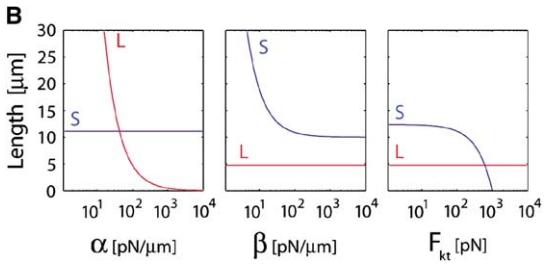

Figure B. Parameter Sensitivity Analysis in Steady State

From these equations, it is clear that in order to reach a stable steady state in which spindle length and overlap length remain constant with time (dS/dt = 0, dL/dt = 0), net polymerization and depolymerization must be equal ($V_{poly} = V_{depol}$). The set of assumptions presented above state that polymerization and depolymerization are constant parameters that naturally produce an unstable steady state in which every perturbation to MT polymerization or depolymerization will result in deviations from the steady state. However, our experiments showed that we can perturb only polymerization or depolymerization by RNAi, yet the spindle still reaches a new steady state with a different constant length (e.g., EB1 RNAi decreases V_{poly} but probably not V_{depol}).

To generate a stable steady state, we propose an additional assumption that the depolymerization rate (V_{depol}) is dependent on the extent of the sliding force ($F_{sliding}$). Here, we proposed one plausible mechanism to explain this dependency on the basis of the assumption of a higher concentration of Klp10A at the centrosomes than elsewhere, combined with a polymer ratchet theory [B8]. If a force of magnitude $F_{sliding}$ pushes MT toward the centrosome, then, as a result of Brownian motion, the probability density for the minus end to be at distance x away from the centrosome is $e^{-\frac{F_{sliding}x}{Nk_bT}}$, where k_bT is the thermal energy [B9] and N is the number of antiparallel overlapping MTs. The implicit assumption here is that the sliding force per single MT is the arithmetic mean, $\frac{F_{sliding}}{N}$, and we are not taking into account differences between different MT populations. Integrating this probability density from 0 to δ, we get the probability that this MT end is not farther than distance δ from the depolymerizing motor: $P(x<\delta) = 1 - e^{-\frac{F_{sliding}\delta}{Nk_bT}}$. Denoting $V_{dep,\,\max}$ as the maximal depolymerization rate, we arrive at the equation:

$$V_{depol} = V_{d,\,0} + V_{dep,\,\max}\left(1 - e^{-\frac{F_{sliding}\delta}{Nk_bT}}\right) = V_{d,0} + V_{dep,\,\max}\left(1 - e^{-\delta\alpha L\left[1 - \frac{V_{sliding}}{V_{sliding,\,\max}}\right] \Big/ Nk_bT}\right) \quad (7)$$

Here we define $V_{d,\,0}$ as sliding-force-independent basal depolymerization at the pole. Our FSM/kymograph analysis of GFP-tubulin suggests that this is

Continued on following page

above zero but also is much smaller than $V_{dep,\,max}$ (Figure S5). It is clear from equation 7 that on the basis of the analysis above, the depolymerization rate is dependent on the overlap region, and its inclusion is sufficient to allow a stable steady-state solution for the basic kinematic force-balance equations (1–3). Substituting all forces (equations 4–6) and the depolymerization term (equation 7) into the basic model (equation 1–3), we get:

$$\frac{dL}{dt} = 2\left(V_{poly} - V_{sliding}\right) \tag{8}$$

$$\frac{dS}{dt} = \mu^{-1} 2\left(\alpha L\left(1 - \frac{V_{sliding}}{V_{sliding,\,max}}\right) - F_{kt,\,0} - \beta(S - S_0)\right) \tag{9}$$

$$V_{sliding} = \frac{1}{2}\frac{dS}{dt} + V_{d,\,0} + V_{dep,\,max}\left(1 - e^{-\delta\alpha L\left(1 - \frac{V_{sliding}}{V_{sliding,\,max}}\right) \Big/ Nk_bT}\right) \tag{10}$$

Solving for S and L at steady state ($dS/dt = 0$, $dL/dt = 0$), we get:

$$S = \frac{\delta(\beta S_0 - F_{kt,\,0}) - \log\left(1 - \frac{V_{poly} - V_{d,\,0}}{V_{dep,\,max}}\right) N \cdot k_b T}{\delta\beta} \tag{11}$$

$$L = \frac{\log\left(1 - \frac{V_{poly} - V_{d,\,0}}{V_{dep,\,max}}\right) K_b T \cdot N}{\delta\alpha\left(\frac{V_{poly}}{V_{sliding,\,max}} - 1\right)} \tag{12}$$

Figure B shows the steady-state values of spindle length (S) and overlap zone (L) for changes in the concentration of Kinesin-5 presented as α defined as force per unit overlap (left panel), tension forces presented as β defined as the Hookean-spring constant (middle panel), and kinetochore forces (right panel). This analysis is based on estimates of numerical values of unknown parameters (Table S4). However, the sensitivity analysis shows that although the exact length can change as a result of changes in the parameter values used, the existence of a solution, and therefore the existence of a stable metaphase steady-state length, is guaranteed (see below, Figure B).

One prediction of this model is that the overlap length (L) is sensitive to the level of Kinesin-5 activity (α). Sensitivity analysis (Figure B) shows that L changes with alteration of Kinesin-5 concentration (fluctuation in sliding force is buffered by changing L), whereas spindle length (S) is independent of Kinesin-5 concentration, as we have documented experimentally in this paper. However, at very low values of α (low concentration of Kinesin-5), the overlap length of antiparallel MTs needs to be greater than the total spindle length in order to maintain outward sliding force, and this is unrealistic in vivo. In the sensitivity graph for α, this ultrasensitive transition can be seen as the intersection between L and S lines (Figure B, left panel). Our model predicts that there is no realistic solution to maintain bipolarity below a certain value of α (or above a certain value of F_{kt}). We interpret that this situation would lead spindles to another stable state—a monopolar spindle. This prediction agrees with our experimental result shown in Figure 4, in which monopolar spindles are exclusively seen at low concentrations of Kinesin-5, but bipolar spindle length is insensitive to high levels of Kinesin-5. The numerical value of this critical threshold of α is 15 pN/μm, based on our selected parameters (Table S4), and represents 15% of the assumed force density of the sliding force in the spindle ($\sim$100 [pN/μm]).

Finally, in metaphase steady state, MT polymerization rate at the kinetochore must also be equal to MT depolymerization rate at the pole. However, the mechanism of this regulation in vivo is unknown, and we did not consider in our modeling. One possibility might be that a similar coupling assumption, in which sliding force of kMTs is coupled with the rates of kMT plus-end polymerization and minus-end depolymerization, allows a steady-state solution.

Box References

B1. Brust-Mascher, I., Civelekoglu-Scholey, G., Kwon, M., Mogilner, A., and Scholey, J.M. (2004). Model for anaphase B: Role of three mitotic motors in a switch from poleward flux to spindle elongation. Proc. Natl. Acad. Sci. USA *101*, 15938–15943.

B2. Margolis, R.L., and Wilson, L. (1981). Microtubule treadmills—possible molecular machinery. Nature *293*, 705–711.

B3. Hill, T.L. (1985). Theoretical problems related to the attachment of microtubules to kinetochores. Proc. Natl. Acad. Sci. USA *82*, 4404–4408.

B4. Sharp, D.J., Brown, H.M., Kwon, M., Rogers, G.C., Holland, G., and Scholey, J.M. (2000). Functional coordination of three mitotic motors in Drosophila embryos. Mol. Biol. Cell *11*, 241–253.

B5. Grill, S.W., Howard, J., Schaffer, E., Stelzer, E.H., and Hyman, A.A. (2003). The distribution of active force generators controls mitotic spindle position. Science *301*, 518–521.

B6. Labbe, J.C., McCarthy, E.K., and Goldstein, B. (2004). The forces that position a mitotic spindle asymmetrically are tethered until after the time of spindle assembly. J. Cell Biol. *167*, 245–256.

B7. Goshima, G., and Vale, R.D. (2003). The roles of microtubule-based motor proteins in mitosis: Comprehensive RNAi analysis in the Drosophila S2 cell line. J. Cell Biol. *162*, 1003–1016.

B8. Peskin, C.S., and Oster, G.F. (1995). Force production by depolymerizing microtubules: Load-velocity curves and run-pause statistics. Biophys. J. *69*, 2268–2276.

B9. Mogilner, A., Elston, T., Wang, H.Y., and Oster, G.F. (2002). Molecular Motors in Computational Cell Biology (New York: Springer).

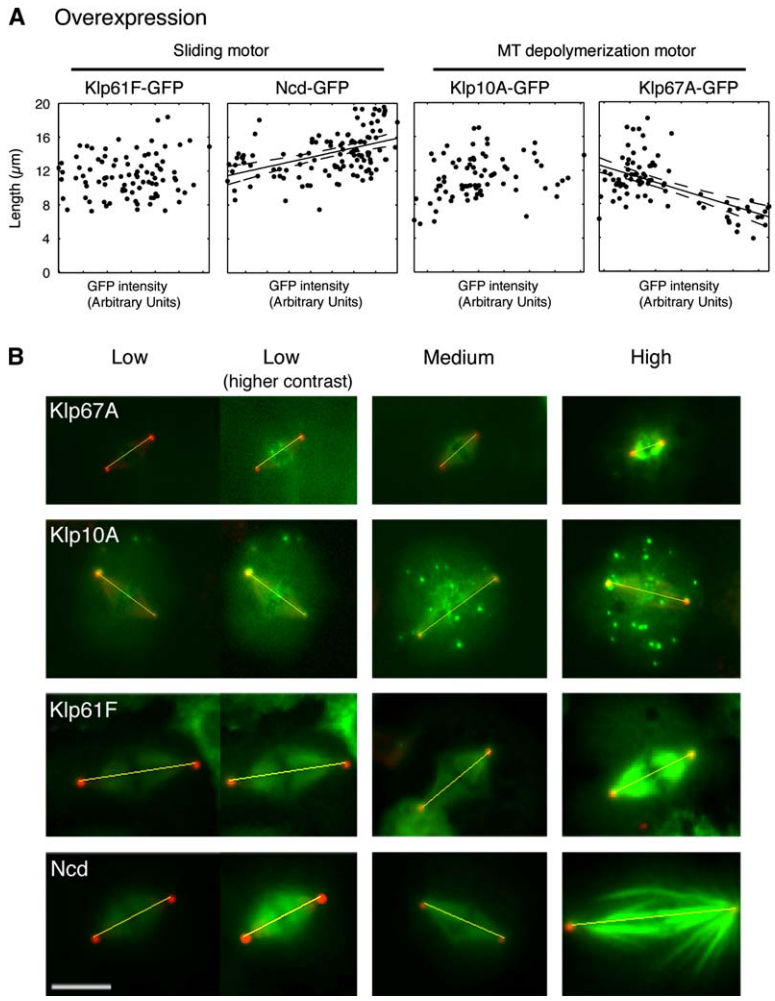

Figure 3. Metaphase Spindle Length after Overexpression of Motor Proteins

(A) Samples scatter plots of overexpression of four GFP-tagged kinesins. Scatter plots show the relationship between protein level (quantified as GFP intensity) and spindle length. Treatments were repeated two, four, four, and six times for Klp67A, Klp10A, Ncd, and Klp61F, respectively. Representative experiments are shown in this panel (see Figure S3 and Table S2 for additional data). No significant correlation was observed between Klp61F and Klp10A levels and spindle length. The correlation between Ncd and Klp67A overexpression and spindle length is significant within the 95% confidence level after Bonferroni correction for multiplicity (see Supplemental Experimental Procedures). In the cases where the correlation was significant, the regression line (continuous) and the 95% confidence interval for the regression line (dashed) are plotted.

(B) Three different levels of overexpression for Klp67A-GFP, Klp10A-GFP, Klp61F-GFP, and Ncd-GFP. Overexpressed Klp67A-GFP, Klp61F-GFP, and Ncd-GFP primarily targeted to the kinetochore or MTs, where endogenous proteins are localized (see higher contrast/brightness panels), whereas cytoplasmic accumulation was detected after Klp10A-GFP overexpression. The bar represents 10 μm. Red shows γ-tubulin, and green shows GFP.

to the main body of the mitotic spindle, as is true of the endogenous motors (Figure 3B). Klp10A-GFP localized primarily to centrosomes/centromeres when expressed at low levels, although cytoplamic accumulation was also detected after overexpression (Figure 3B). Therefore, overexpression of Klp10A-GFP might not result in increased motor concentrations at spindle poles. Figure 3A reveals that expression of the MT depolymerase, Klp67A, caused a dose-dependent shortening of the metaphase spindle (more data sets are available in Figure S3 and Table S2). In contrast, overexpression of Klp10A-GFP did not result in a statistically significant change in metaphase spindle length in our overexpression range (Figure 3A). Surprisingly, overexpression of Ncd caused a statistically significant dose-dependent elongation of the metaphase spindle in two out of four experiments (Figure 3A). This result is opposite to that expected from prior results and models implicating Ncd as a motor that generates an inward force on antiparallel MTs [5, 6, 8]. However, an in vitro study shows that the MT binding domain within the nonmotor region of Ncd can induce MT nucleation, stabilization, and bundling [32], so the length increase may be attributed to MT-stabilizing effects of motor overxpression (Figure 3B). Perhaps the biggest surprise was the lack of correlation between Klp61F-GFP expression level and spindle length in six independent experiments (Figure 3A, Figure S3, and Table S2). Thus, in contrast to previous results obtained in yeast [5], we conclude that the overexpression of the sliding motor Klp61F has no effect on spindle length in S2 cells.

To better understand how balances of forces might govern spindle length, we developed a preliminary quantitative model (described in detail in Box 1). This quantitative analysis is based on several plausible but unproven assumptions. First, on the basis of a linear force-balance curve, we assumed that MT sliding forces are proportional to forces applied by Kinesin-5. Second, we assumed that the spindle elastic properties can be approximated by a Hookean spring. Third, sister chromatids are under tension at the kinetochores, in which pulling force generated by antiparallel MT sliding and/or MT depolymerization at the poles is opposed by sister-chromatid cohesion. To test whether the third assumption is relevant in S2 cells, we measured sister-kinetochore distance as a maker of sister-chromatid tension, where longer distance ("stretched" centromeres) represents a stronger pulling force at the kinetochore by kMTs [33]. By immunofluorescence of Cid (*Drosophila* CENP-A, histone H3 variant that localizes to inner kinetochores), we found, consistent with previous reports [30, 34], that sister-kinetochore distance during

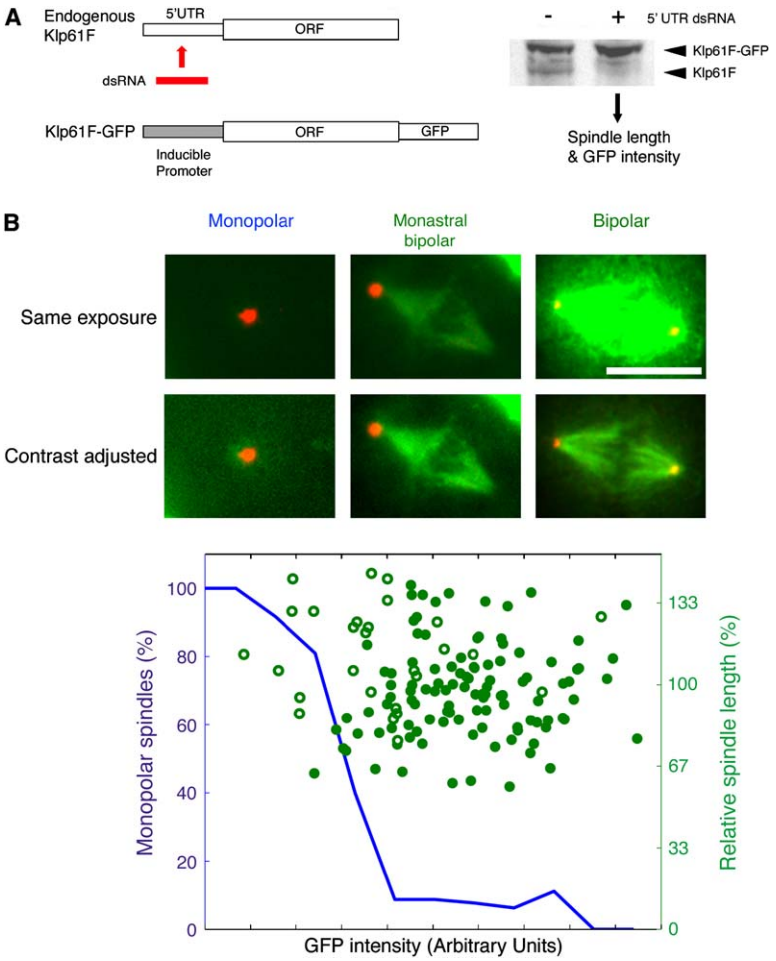

Figure 4. Bistability of the Spindle Morphology but Robustness of Metaphase Spindle Length to Alteration of Kinesin-5 Concentration

(A) RNAi knockdown of endogenous Klp61F with dsRNA targeting 5′ UTR region was combined with ectopic expression of Klp61F-GFP. Immunoblot was performed by anti-Klp61F antibody.

(B) Spindle "bistability." At top, representative images of monopolar, monastral bipolar, and bipolar spindles are shown. Red shows γ-tubulin, and green shows Klp61F-GFP. The bar represents 10 μm. At bottom, frequency of monopolar spindles over total monopolar and normal bipolar spindles is shown by blue line; frequency was calculated on the basis of the distribution of 238 spindles into 15 bins. Length distributions of the normal bipolar spindle (green dots) and monastral bipolar spindle (green open circles; γ-tubulin staining at only one pole of the bipolar spindle) after various levels of Klp61F-GFP expression are also plotted. Abrupt decrease in monopolar spindle frequency is observed at a critical expression level of Klp61F. The length of monastral bipolar spindles was measured by doubling the distance between γ-tubulin and center of the chromosome mass.

metaphase is 25% longer (1.0 ± 0.13 μm [n = 23], $p < 0.0001$) than in colchicine-treated cells, which lack kMT tension (0.8 ± 0.13 μm [n = 47]) (Figure S4A). Time-lapse imaging of Klp67A-GFP (as an outer-kinetochore marker) also showed that metaphase sister-kinetochore distance rapidly decreased upon colchicine treatment (n = 6, Figure S4B, Movie S1). These data support the idea that sister kinetochores are under tension during metaphase in S2 cells.

Combining these forces via a simple force-balance model [13], we show that these assumptions by themselves are not sufficient to allow a stable metaphase steady-state (Box 1). We further tested what other assumptions allow the steady state to be achieved. We found that the addition of an assumption that the rate of MT depolymerization at spindle poles (which contributes to poleward flux [1, 4, 35]) is proportional to the motor-generated sliding forces is sufficient to allow stability of the metaphase steady state [Box 1, equation (7)]. This feature also enables the spindle length to remain constant despite the overexpression of the Kinesin-5 motor. Although this assumption remains speculative in *Drosophila* cells, it is supported by recent experiments showing that the rate of poleward flux in meiotic spindles assembled in *Xenopus* extracts correlates with Kinesin-5 activity in a dose-dependent manner [18]. Kinesin-5 activity also appears to be an important factor in maintaining spindle bipolarity and generating poleward flux in S2 cells because RNAi of Klp61F (Kinesin-5) causes a bipolar-to-monopolar spindle collapse and a concomitant significant reduction in the rate of poleward flux (Figure S5, Movies S2 and S3). Given these assumptions, the quantitative model explains how changing the rate of MT polymerization/depolymerization can produce changes in the metaphase spindle length without changing its stability while the length can remain insensitive to a wide range of Kinesin-5 concentration.

A novel outcome of our model is that it predicts "bistability" in spindle architecture. Specifically, at low concentrations of Klp61F (Kinesin-5), monopolar spindles are created, but as the concentration of this motor increases, an abrupt transition to bipolar spindle formation takes place [Box 1, equation (11) and Figure B]. To test this prediction of spindle bistability, we examined the relationship between Klp61F expression and spindle length over a wide range of motor concentrations by RNAi-depleting endogenous Klp61F by using dsRNA directed against its 5′ UTR and then expressing varying levels of Klp61F-GFP from a plasmid with an inducible promoter (Figure 4A and [22]). We assume that the expressed fusion protein is active, an assumption that is supported by its ability to rescue bipolar spindle assembly in RNAi-treated cells at appropriate concentrations (Figure 4B). Significantly, we found that there was an abrupt increase in the percentage of cells that exhibited bipolar spindles at a critical level of Klp61F-GFP protein

expression (Figure 4B, blue line) and that the length of the bipolar spindle was uniform above this critical level (Figure 4B, solid green dots). In addition, we frequently observed bipolar spindles with a single γ-tubulin signal at only one pole ("monastral bipolar spindle") near the critical expression level of Klp61F. Our previous work demonstrated that monastral bipolar spindles are generated by a pathway in which monopolar spindles initially form and then a second pole forms by MT generation from the chromosomes followed by their focusing to form an acentrosomal pole [3]. The length of the monastral bipolar spindles at low Klp61F-GFP levels (measured by doubling the distance between γ-tubulin and the metaphase plate) was also similar to normal bipolar spindles (Figure 4B, green circles). This experiment demonstrates both the sharp monopolar-to-bipolar spindle transition that occurs with increasing Kinesin-5 concentration and the robust maintenance of bipolar spindle length above this critical Kinesin-5 concentration. The latter result also supports our conclusion from the overexpresssion data that bipolar spindle length is relatively insensitive to changes in Klp61F concentration in S2 cells.

Conclusions

In summary, our quantitative analyses indicate that MT dynamics are the major determinants of metaphase spindle length, with MT sliding playing a relatively minor role in determining length. Sister-chromatid cohesion is also critical to restrain the length. Our model also provides a possible explanation for the surprising insensitivity of spindle length to sliding forces. This model uses a simple set of force-balance equations [13] combined with a "coupling assumption" in which increasing motor-driven forces leads to faster rates of depolymerization of MTs. The sliding-depolymerization-coupling model also might explain the difference between our results, showing no change in spindle length with varying Kinesin-5 levels, and those in yeast, where varying the concentration of this motor affects spindle length [5, 7]. Unlike metazoan cells, budding yeast displays no detectable MT depolymerization at spindle poles [36] and thus may lack a means of buffering spindle length in response to pushing effects of microtubule motors. Undoubtedly, aspects of the model will need to be revised, and additional parameters will need to be incorporated (e.g., astral microtubule forces are not considered here). Nevertheless, the model in its present state has already served to predict a "bistabilty" in spindle morphology in which a threshold amount of Kinesin-5-generated force is needed to prevent spindle collapse. With a combination of RNAi and protein overexpression, this prediction was experimentally verified. The model may make other predictions that could be explored in the future. For example, the model predicts that the degree of central-spindle MT overlap (L) varies in response to Kinesin-5 levels (Box 1, Figure B), which could be examined in the future by 3D reconstructions of the spindle by electron or deconvolusion microscopy. As another example, a polymer ratchet mechanism was incorporated to explain sliding-depolymerization coupling (Box 1 equation (7)). Such a coupling could be achieved by a gradient of the Klp10A MT depolymerase activity at the spindle poles [4], which would allow stronger sliding forces generated by Klp61F to push MT minus ends farther into the interior region of the pole, where the depolymerase activity might be correspondingly higher. Thus, our current model, although not providing a final answer to how mitotic spindle length is controlled and buffered in response to changing forces, provides a useful framework for additional experimentation and more detailed modeling of this important problem in the future.

Supplemental Data

Supplemental Data include Supplemental Experimental Procedures, five Supplemental Figures, four Supplemental Tables, and three Supplemental Movies and are available with this article online at: http://www.current-biology.com/cgi/content/full/15/22/1979/DC1/.

Acknowledgments

This project originated at the Physiology Course at the Marine Biological Laboratory at Woods Hole. We are grateful to Axon Instrument for the use of their ImageXpress microscopic system, Olivia George and Prabhat Kunwar for their help in the early stage of this work in Physiology Course, and all the members of Physiology Course 2004 at MBL for stimulating discussion. We are also grateful to Alex Mogilner and Gul Civelekoglu-Scholey for valuable suggestions on mathematical modeling; Reed Kelso for the help of data analysis; and Nicole Mahoney, Steve Rogers, Steve Henikoff, and Jordan Raff for the gift of reagents. G.G. is the recipient of a postdoctoral fellowship from Human Frontier Science Program Organization (HFSPO).

Received: May 20, 2005
Revised: September 13, 2005
Accepted: September 30, 2005
Published: November 21, 2005

References

1. Inoue, S., and Salmon, E.D. (1995). Force generation by microtubule assembly/disassembly in mitosis and related movements. Mol. Biol. Cell *6*, 1619–1640.
2. Gorbsky, G.J., Simerly, C., Schatten, G., and Borisy, G.G. (1990). Microtubules in the metaphase-arrested mouse oocyte turn over rapidly. Proc. Natl. Acad. Sci. USA *87*, 6049–6053.
3. Goshima, G., and Vale, R.D. (2003). The roles of microtubule-based motor proteins in mitosis: Comprehensive RNAi analysis in the Drosophila S2 cell line. J. Cell Biol. *162*, 1003–1016.
4. Rogers, G.C., Rogers, S.L., Schwimmer, T.A., Ems-McClung, S.C., Walczak, C.E., Vale, R.D., Scholey, J.M., and Sharp, D.J. (2004). Two mitotic kinesins cooperate to drive sister chromatid separation during anaphase. Nature *427*, 364–370.
5. Saunders, W., Lengyel, V., and Hoyt, M.A. (1997). Mitotic spindle function in Saccharomyces cerevisiae requires a balance between different types of kinesin-related motors. Mol. Biol. Cell *8*, 1025–1033.
6. Sharp, D.J., Brown, H.M., Kwon, M., Rogers, G.C., Holland, G., and Scholey, J.M. (2000). Functional coordination of three mitotic motors in Drosophila embryos. Mol. Biol. Cell *11*, 241–253.
7. Straight, A.F., Sedat, J.W., and Murray, A.W. (1998). Time-lapse microscopy reveals unique roles for kinesins during anaphase in budding yeast. J. Cell Biol. *143*, 687–694.
8. Troxell, C.L., Sweezy, M.A., West, R.R., Reed, K.D., Carson, B.D., Pidoux, A.L., Cande, W.Z., and McIntosh, J.R. (2001). pkl1(+)and klp2(+): Two kinesins of the Kar3 subfamily in fission yeast perform different functions in both mitosis and meiosis. Mol. Biol. Cell *12*, 3476–3488.
9. Gaetz, J., and Kapoor, T.M. (2004). Dynein/dynactin regulate metaphase spindle length by targeting depolymerizing activities to spindle poles. J. Cell Biol. *166*, 465–471.
10. Goshima, G., Saitoh, S., and Yanagida, M. (1999). Proper metaphase spindle length is determined by centromere proteins Mis12 and Mis6 required for faithful chromosome segregation. Genes Dev. *13*, 1664–1677.

11. Garcia, M.A., Koonrugsa, N., and Toda, T. (2002). Two kinesin-like Kin I family proteins in fission yeast regulate the establishment of metaphase and the onset of anaphase A. Curr. Biol. *12*, 610–621.
12. Cytrynbaum, E.N., Scholey, J.M., and Mogilner, A. (2003). A force balance model of early spindle pole separation in Drosophila embryos. Biophys. J. *84*, 757–769.
13. Brust-Mascher, I., Civelekoglu-Scholey, G., Kwon, M., Mogilner, A., and Scholey, J.M. (2004). Model for anaphase B: Role of three mitotic motors in a switch from poleward flux to spindle elongation. Proc. Natl. Acad. Sci. USA *101*, 15938–15943.
14. Nedelec, F. (2002). Computer simulations reveal motor properties generating stable antiparallel microtubule interactions. J. Cell Biol. *158*, 1005–1015.
15. Vass, S., Cotterill, S., Valdeolmillos, A.M., Barbero, J.L., Lin, E., Warren, W.D., and Heck, M.M. (2003). Depletion of Drad21/Scc1 in Drosophila cells leads to instability of the cohesin complex and disruption of mitotic progression. Curr. Biol. *13*, 208–218.
16. Rogers, S.L., Rogers, G.C., Sharp, D.J., and Vale, R.D. (2002). Drosophila EB1 is important for proper assembly, dynamics, and positioning of the mitotic spindle. J. Cell Biol. *158*, 873–884.
17. Maiato, H., Sampaio, P., Lemos, C.L., Findlay, J., Carmena, M., Earnshaw, W.C., and Sunkel, C.E. (2002). MAST/Orbit has a role in microtubule-kinetochore attachment and is essential for chromosome alignment and maintenance of spindle bipolarity. J. Cell Biol. *157*, 749–760.
18. Miyamoto, D.T., Perlman, Z.E., Burbank, K.S., Groen, A.C., and Mitchison, T.J. (2004). The kinesin Eg5 drives poleward microtubule flux in Xenopus laevis egg extract spindles. J. Cell Biol. *167*, 813–818.
19. Dujardin, D.L., and Vallee, R.B. (2002). Dynein at the cortex. Curr. Opin. Cell Biol. *14*, 44–49.
20. Brittle, A.L., and Ohkura, H. (2005). Mini spindles, the XMAP215 homologue, suppresses pausing of interphase microtubules in Drosophila. EMBO J. *24*, 1387–1396. Published online March 17, 2005. 10.1038/sj.emboj.7600629.
21. Maiato, H., Khodjakov, A., and Rieder, C.L. (2005). Drosophila CLASP is required for the incorporation of microtubule subunits into fluxing kinetochore fibres. Nat. Cell Biol. *7*, 42–47.
22. Goshima, G., and Vale, R.D. (2005). Cell cycle-dependent dynamics and regulation of mitotic kinesins in Drosophila S2 cells. Mol. Biol. Cell *16*, 3896–3907.
23. Gandhi, R., Bonaccorsi, S., Wentworth, D., Doxsey, S., Gatti, M., and Pereira, A. (2004). The Drosophila kinesin-like protein KLP67A is essential for mitotic and male meiotic spindle assembly. Mol. Biol. Cell *15*, 121–131.
24. Savoian, M.S., Gatt, M.K., Riparbelli, M.G., Callaini, G., and Glover, D.M. (2004). Drosophila Klp67A is required for proper chromosome congression and segregation during meiosis I. J. Cell Sci. *117*, 3669–3677.
25. Cullen, C.F., Deak, P., Glover, D.M., and Ohkura, H. (1999). mini spindles: A gene encoding a conserved microtubule-associated protein required for the integrity of the mitotic spindle in Drosophila. J. Cell Biol. *146*, 1005–1018.
26. Goshima, G., Nedelec, F., and Vale, R.D. (2005). Mechanisms for focusing mitotic spindle poles by minus-end-directed motor proteins. J. Cell Biol. *171*, 229–240.
27. Scholey, J.M., Rogers, G.C., and Sharp, D.J. (2001). Mitosis, microtubules, and the matrix. J. Cell Biol. *154*, 261–266.
28. Mitchison, T.J., Maddox, P., Gaetz, J., Groen, A., Shirasu, M., Desai, A., Salmon, E.D., and Kapoor, T.M. (2005). Roles of polymerization dynamics, opposed motors and a tensile element in governing the length of Xenopus extract meiotic spindles. Mol. Biol. Cell *16*, 3064–3076. Published online March 23, 2005. 10.1091/mbc.E05-02-0174.
29. Heald, R., Tournebize, R., Habermann, A., Karsenti, E., and Hyman, A. (1997). Spindle assembly in Xenopus egg extracts: Respective roles of centrosomes and microtubule self-organization. J. Cell Biol. *138*, 615–628.
30. Maiato, H., Rieder, C.L., and Khodjakov, A. (2004). Kinetochore-driven formation of kinetochore fibers contributes to spindle assembly during animal mitosis. J. Cell Biol. *167*, 831–840.
31. Morales-Mulia, S., and Scholey, J.M. (2005). Spindle pole organization in Drosophila S2 cells by dynein, abnormal spindle protein (Asp), and KLP10A. Mol. Biol. Cell *16*, 3176–3186.
32. Karabay, A., and Walker, R.A. (1999). The Ncd tail domain promotes microtubule assembly and stability. Biochem. Biophys. Res. Commun. *258*, 39–43.
33. Waters, J.C., Skibbens, R.V., and Salmon, E.D. (1996). Oscillating mitotic newt lung cell kinetochores are, on average, under tension and rarely push. J. Cell Sci. *109*, 2823–2831.
34. Logarinho, E., Bousbaa, H., Dias, J.M., Lopes, C., Amorim, I., Antunes-Martins, A., and Sunkel, C.E. (2004). Different spindle checkpoint proteins monitor microtubule attachment and tension at kinetochores in Drosophila cells. J. Cell Sci. *117*, 1757–1771.
35. Desai, A., Maddox, P.S., Mitchison, T.J., and Salmon, E.D. (1998). Anaphase A chromosome movement and poleward spindle microtubule flux occur At similar rates in Xenopus extract spindles. J. Cell Biol. *141*, 703–713.
36. Maddox, P.S., Bloom, K.S., and Salmon, E.D. (2000). The polarity and dynamics of microtubule assembly in the budding yeast Saccharomyces cerevisiae. Nat. Cell Biol. *2*, 36–41.